Estimation of Propagation Losses for Narrow Strip and Rib Waveguides

Susan M. Lindecrantz, *Member, IEEE*, and Olav Gaute Hellesø, *Member, IEEE*

***Abstract*— The dependence of propagation losses on waveguide width and polarization is measured for strip and rib waveguides made of tantalum pentoxide. For strip waveguides, the propagation losses are found to increase rapidly for widths <3 μm. The losses were significantly smaller for rib than for strip waveguides, as expected. A method is developed for estimating the dependence of propagation losses on waveguide width. The method is based on approximating sidewall imperfections with an area with complex refractive index in a 2D model and showed a good agreement with the measured dependence on waveguide width. The method is also used to predict that propagation losses will decrease rapidly for rib heights less than 20 nm for TM-polarization.**

***Index Terms*— Strip waveguide, rib waveguide, propagation loss, sidewall roughness, scattering loss, tantalum pentoxide.**

I. Introduction

IN ORDER to tightly confine light in optical waveguides, the refractive index of the core must be high and the cross-section of the waveguide must be small. At the same time, propagation losses must be kept low to allow complex optical circuits. The main sources of propagation loss for a dielectric straight waveguide are absorption within the materials and radiation losses from imperfections in the materials and on the sidewalls [1]. As the refractive index is increased and the cross-section reduced, the imperfections of the sidewalls become the dominating source of propagation losses. In this letter, the influence of the height of the sidewalls (i.e. rib height) and the waveguide width on propagation losses is studied experimentally and simulated.

Propagation losses are of general importance for integrated optics. The wavelength, waveguide structure and materials used in this letter are particularly relevant for evanescent field sensors, e.g. based on the Mach-Zehnder waveguide interferometer. Two commonly used materials for waveguide sensors and biosensors are Si_3N_4 [2], [3] and Ta_2O_5 [4]. These materials are transparent in the visible and near infrared, and have a refractive index of 2 and 2.1, respectively. For the experimental work, we have chosen Ta_2O_5 and the corresponding refractive index is used for the simulations. For evanescent field sensors, the sensitivity increases with the refractive index of the core and with decreasing core thickness [5]–[7]. For the Mach-Zehnder interferometer, it is imperative that the waveguides are single-mode. This can be obtained by reducing the width of the waveguide or by using rib waveguides where the core is only partially etched down on the sides. Shallow rib waveguides with 4 nm rib height, widths of 3-4 μm and 200 nm core thickness have been made with propagation losses as low as 0.15 dB/cm for TE-polarization and 0.30 dB/cm for TM-polarization [8].

Several methods exist to estimate propagation losses from surface roughness, see [9]–[11]. These methods require parameters such as the roughness standard deviation and the autocorrelation length of the sidewall roughness to be known. Surface roughness is usually measured using atomic force microscopy (AFM). For narrow waveguides, the critical parameter is the sidewall roughness, rather than the surface roughness. However, it is a challenge to measure the sidewall roughness for strip waveguides (200 nm high sidewalls) and very difficult for shallow rib waveguides (1-10 nm high sidewalls). Rather than basing the simulations on roughness measurements, we have used a measured propagation loss for a narrow waveguide as a reference to estimate the propagation loss for other waveguide widths. Our method is based on approximating the surface roughness with a small section with complex refractive index in a 2D model. The method is described in the next section and it is tested on strip and rib waveguides.

II. Methods

A. Experimental Methods

Strip and rib waveguides were produced by sputtering a core layer of tantalum pentoxide ($n_{core} = 2.15$) onto a 5 μm silica layer (n = 1.45). The waveguides were defined by photolithography followed by argon ion-beam milling at an angle of 45° to reduce the sidewall roughness. The waveguides were treated with plasma-ashing for 10 minutes to remove remaining photoresist and annealed at 450 °C-600 °C in oxygen in a tube furnace for 2-5 hours [12]. Rib waveguides were made with a core thickness, H, of 170 nm and a slab thickness, h, of 150 nm, see Fig. 1. The strip waveguides had a core thickness, H, of 215 nm and by definition a slab thickness h = 0. These dimensions have been determined using a scanning electron microscope (SEM) and a mechanical profiler (Tencor P6).

The propagation losses were measured for w = 1-10 μm wide strip waveguides and w = 1-5 μm wide rib waveguides. Light from a 785 nm diode laser was coupled into the waveguide using beam expanding lenses and a 40× objective lens. The polarization was rotated with a half-wave plate

Manuscript received March 12, 2014; revised May 2, 2014; accepted July 4, 2014. Date of publication July 9, 2014; date of current version August 15, 2014. This work was supported by the Research Council of Norway.

The authors are with the Department of Physics and Technology, UiT - The Arctic University of Norway, Tromsø 9037, Norway (e-mail: susan.lindecrantz@uit.no; olav.gaute.helleso@uit.no).

Color versions of one or more of the figures in this letter are available online at http://ieeexplore.ieee.org.

Digital Object Identifier 10.1109/LPT.2014.2337055

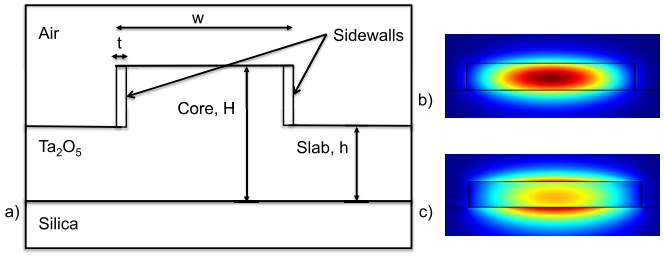

Fig. 1. a) Schematic diagram of the waveguide cross-section used in Comsol simulations (not to scale). Examples of the fundamental mode for a strip waveguide for b) TE- and c) TM-polarization.

to obtain TE- or TM-polarization. A second 40× objective lens was used to couple light out from the waveguide into a photodetector. The photodetector was used to ensure that optimal and stable coupling was obtained during the measurements.

The propagation losses were measured by taking images of light scattered from the waveguide with a microscope on a translation stage. The microscope was moved along the waveguide and images of the scattered light captured. This is a non-destructive method independent of input coupling and suitable for measurement of relatively high propagation losses (dB/cm-range) [1], [13], [14]. The images of scattered light were captured with an objective lens with a relatively large magnification, 50×, and NA = 0.8, in order to avoid interference between scattering points and to limit the area observed. The exposure time for the microscope's CCD camera was adjusted to the maximum time not giving saturated points in the image. The images were processed with a Matlab-program. For each image, the pixels were summed along the waveguide, giving an approximately Gaussian profile across the waveguide. Pixels within the FWHM-width of the profile were subsequently summed along and across the waveguide, giving a relative intensity for the image. This value was corrected for the exposure time, i.e. by dividing by the exposure time. The first image, taken near the input, was used as a reference and given the value $I(0) = 0$ dB. Images captured further from the input thus gave intensities $I(z)$, with intensity in dB and distance z measured from the position of the reference image.

Fig. 2 shows an example of the measured scattering as function of the propagation distance. The images are taken of scattering from randomly distributed imperfections, mostly on the waveguide surface. The measured intensities will thus have a statistical variation. A straight line was fitted to the data with the least-squares method. The slope was used to find the propagation loss and the standard deviation of the slope was used to characterize the statistical variation. For the case in Fig. 2, this gave a propagation loss of 6.7 ± 1.6 dB/cm.

For relatively wide waveguides, i.e. 5-10 μm for strip waveguides and 3-5 μm for rib waveguides, the propagation losses do not depend on width as seen in Fig. 3. Thus, propagation losses for these wide waveguides are less dependent on scattering from the sidewalls and mostly due to absorption and scattering from imperfections within the material. The average propagation loss is 1.4 dB/cm and 1.3 dB/cm for TE-polarization and 1.1 dB/cm and 1.5 dB/cm for

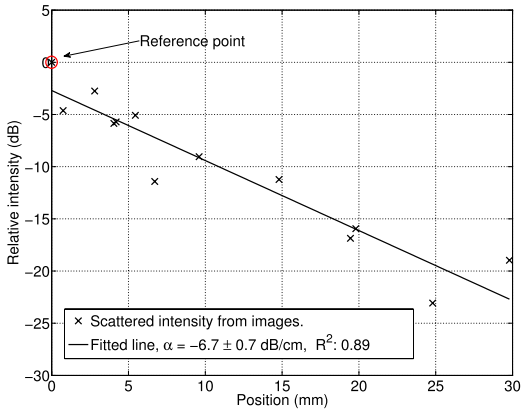

Fig. 2. Relative scattering intensity versus position for strip waveguide of width 1.5 μm and TE-polarization.

TM-polarization for wide strip and rib waveguides, respectively (see Fig. 3 and result-section). This average loss was subtracted from the measured values for all waveguide widths before simulations. The remaining loss, α_{dB}, is taken to be due to scattering from the sidewalls.

B. Simulation of Propagation Losses

Comsol Multiphysics was used to find the complex effective refractive index of waveguides. The sidewalls are represented in the model by an area of width t on each side of the core as shown in Fig. 1. Losses due to scattering from the sidewalls are included in the model by adding an imaginary part to the refractive index for this area. A width $t = 10$ nm was used for the simulations. It was tested that the results where independent of the width t by doing simulations with widths 5 and 20 nm for some cases.

To find the relationship between simulated complex effective refractive index and measured propagation loss, the attenuation coefficient, α_{dB} (in dB/cm), can be written as:

$$\alpha_{dB} = -10 \log (P(z)/P_0) \tag{1}$$

where P_0 is the reference intensity and $P(z)$ is the intensity at distance z from the reference point. The power $P(z)$ is related to the effective refractive index n_{eff} by:

$$P(z) = |U(z)|^2 = |A_0 \exp(-jkz)|^2 = P_0 \exp(\frac{-4\pi}{\lambda_0} n_{im} z) \tag{2}$$

where $U(z)$ is the time-independent complex wavefunction, A_0 is the complex envelope constant, k is the wavevector and λ_0 is the wavelength (785 nm). A propagation loss α_{dB} thus corresponds to an imaginary part n_{im} of the effective refractive index with z = 0.01 m:

$$n_{im} = -\frac{\lambda_0 \alpha_{dB}}{40 z \pi log e} \tag{3}$$

Simulations in COMSOL are done to iteratively find the complex refractive index of the sidewalls, $n_{core} + jn_w$, that gave a complex effective refractive index (for the mode) equal to $n_{re} + jn_{im}$. Here n_{re} is the real part of the effective refractive index and n_{im} corresponds to the measured loss using Eq. 3. The complex value found, $n_{core} + jn_w$, is subsequently used to find the complex effective refractive index,

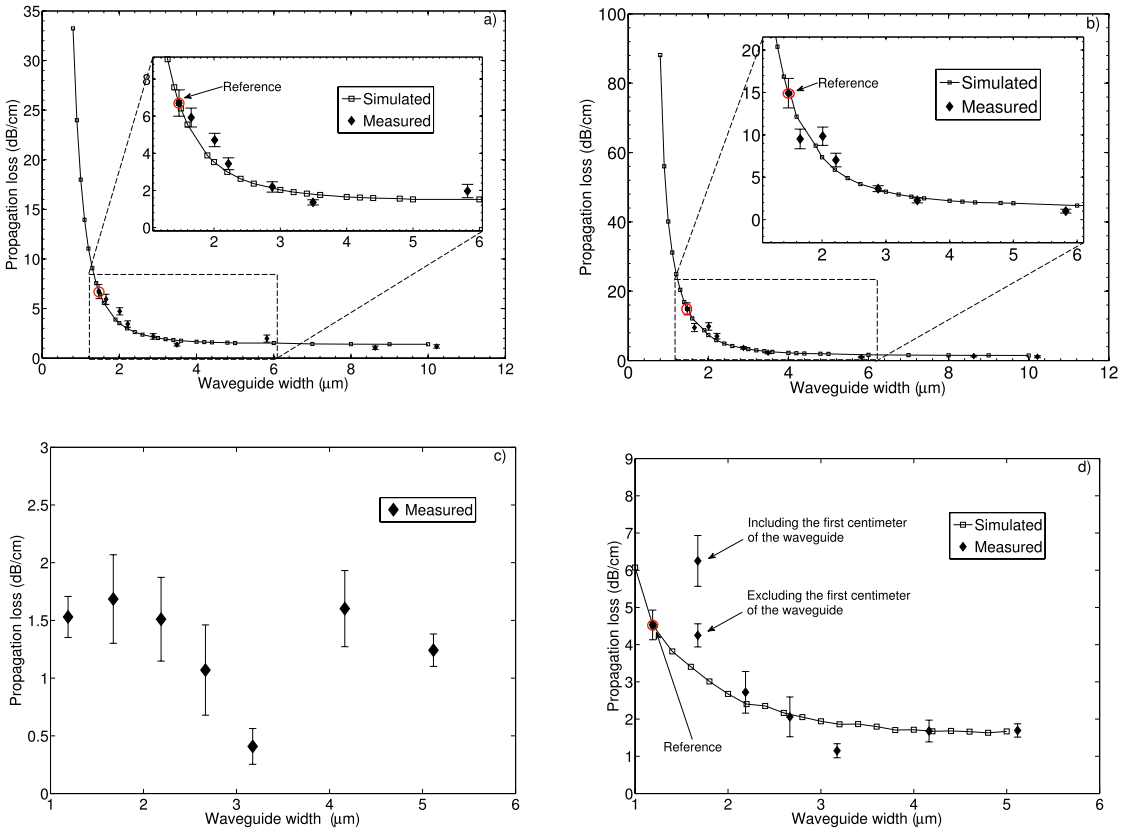

Fig. 3. Propagation losses as function of waveguide width for strip waveguides, for a) TE-polarization and b) TM-polarization. Propagation losses as function of waveguide width for rib waveguides, for c) TE-polarization and d) TM-polarization.

and thus the loss, for other waveguide widths. The selected reference waveguides had a width of 1.5 μm for strip waveguides and 1.2 μm for rib waveguides. The thickness of the waveguides simulated was the same as for the waveguides measured. Care was taken to avoid interference from higher order TE- solutions when simulating TM-polarization. Fig. 1(b) and 1(c) shows examples of simulated fundamental modes for TE- and TM-polarization ($\lambda = 785$ nm).

Our technique assumes that the random and spatially distributed surface roughness can be approximated with a thin layer of constant complex refractive index. Furthermore, the simulation only considers the fundamental mode. For multimode waveguides, higher order modes will have a different spatial distribution and thus be influence differently by the surface roughness compared to the fundamental mode.

III. Results and Discussion

Fig. 3(a) and 3(b) shows the measured and simulated propagation losses for strip waveguides for TE- and TM-polarization. The propagation losses increase very fast as the width decreases below 3 μm. For wider waveguides than 3 μm, the propagation losses show insignificant dependency on the width. The measurement uncertainty is small for these low losses, while for the larger losses of narrow waveguides, the measurement uncertainty also becomes larger. This is most likely due to the random nature of the imperfections, with some sections of the waveguide having low losses and others having large losses. The losses are considerably larger for TM-polarization than for TE-polarization. The simulated propagation losses show good overlap with the measurements. In particular, the simulations predict well the increase in propagation losses around 3μm width. An exponential fit to the data would be possible, but requires at least two reference points, whereas our simulation is based on a single reference point. It also gives a more physical approach to the propagation losses. However, care should be taken when extrapolating to very narrow waveguides. Measured and simulated propagation losses for rib waveguides are shown in Fig. 3(c) and 3(d). As for strip waveguides, the losses of rib waveguides for TM-polarization are larger than for TE-polarization. For TE-polarization, the losses show no significant dependency on waveguide width down to a width of 1.2 μm. For TM-polarization, losses increase rapidly for waveguides less than 3 μm wide. As there was no visible dependency on width for TE-polarization, this case cannot be simulated with our method. For TM-polarization there is good overlap between simulations and measurements. For a width of 1.7 μm, two results are included. The larger value includes measurements on the first 1 cm of the waveguide, while the lower value excludes these. There was a sharp decrease in measured intensity from 0.5 cm to 1 cm, probably cause by a large point defect between these measurements.

Propagation losses for the rib waveguides were, as expected, significantly smaller than for strip waveguides. For a 1.5 μm wide waveguide and TE-polarization, propagation losses

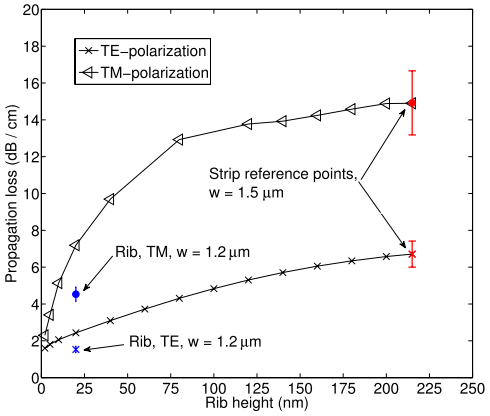

Fig. 4. Simulated propagation loss as function of rib height, $H-h$, based on measured propagation loss for a 1.5 μm wide strip waveguide. Also, measured loss is shown for waveguides with 20 nm rib height and 1.2 μm width.

decreases from 6.7 dB/cm to 1.7 dB/cm when changing from a strip to rib waveguide. To simulate this dependancy on rib height, we have used jn_w found for a strip waveguide, to find the losses for rib waveguides as function of rib height, H-h. In this case, the width was kept fixed at 1.5 μm. The propagation loss is shown in Fig. 4. The measured loss for a waveguide with rib height 20 nm is also shown, with the core thickness 170 nm, versus 215 nm for the strip waveguide.

The simulations show reasonable correspondence with the measured losses for the rib waveguides, given that the measurement uncertainties are large for the reference strip waveguide and the rib waveguides. The simulations predict that propagation losses for TM-polarization can be decreased significantly by reducing the rib height below 20 nm. For TE-polarization, the propagation losses are approximately linear with rib height. For shallow rib waveguides with rib height less than 10 nm, the losses due to sidewall roughness are small and losses from absorption and scattering within the material become dominant, according to our simulations.

IV. Conclusion

The measured propagation losses increased sharply for tantalum pentoxide strip waveguides less than 3 μm wide. For rib waveguides, the propagation losses are significantly smaller than for the strip waveguides. For TE-polarization, the propagation loss was not significantly influenced by the width for rib waveguides. Losses caused by random sidewall imperfections are dependent on fabrication and can vary along a waveguide, as demonstrated in Fig. 3(d) for a width of 1.7 μm. Our simulation method, based on an area with complex refractive index in a 2D-model, gave good estimates for the dependency of propagations losses on waveguide width. The method was also used to estimate the dependency of propagation losses on rib height, showing that losses for TM-polarization decrease fast for rib heights less than 20 nm. For TE-polarization, the losses were predicted to change gradually with rib height.

The measured dependency of propagation losses on waveguide width can, together with the simple proposed simulation method, give valuable information for the design of rib waveguides. The most common way of obtaining single-mode waveguides is to reduce the waveguide width. With the proposed method, it is possible to estimate how the propagation losses will increase when reducing the width for a given technology. The method is based on having several waveguide widths available and the usefulness of the method is thus if considering to reduce the width to even more narrow waveguides than those available. Reducing the rib height is another way of obtaining single-mode waveguides. It is necessary to make several wafers and do more processing to experimentally compare the influence of rib height on propagation losses, while the proposed method can estimate the influence of rib height based on one wafer with a single rib height.

Acknowledgment

The authors would like to thank Dr. Balpreet S. Ahluwalia and Dr. Pål Løvhaugen for helpful inputs.

References

[1] R. G. Hunsperger, *Integrated Optics: Theory and Technology*, vol. 2. New York, NY, USA: Springer-Verlag, 1984.

[2] M.-C. Estevez, M. Alvarez, and L. M. Lechuga, "Integrated optical devices for lab-on-a-chip biosensing applications," *Laser Photon. Rev.*, vol. 6, no. 4, pp. 463–487, 2012.

[3] C. A. Barrios, "Analysis and modeling of a silicon nitride slot-waveguide microring resonator biochemical sensor," *Proc. SPIE*, vol. 7356, pp. 735605-1–735605-10, May 2009.

[4] K. Schmitt, K. Oehse, G. Sulz, and C. Hoffmann, "Evanescent field sensors based on tantalum pentoxide waveguides—A review," *Sensors*, vol. 8, no. 2, pp. 711–738, 2008.

[5] O. Parriaux and G. J. Veldhuis, "Normalized analysis for the sensitivity optimization of integrated optical evanescent-wave sensors," *J. Lightw. Technol.*, vol. 16, no. 4, pp. 573–582, Apr. 1998.

[6] R. G. Heideman and P. V. Lambeck, "Remote opto-chemical sensing with extreme sensitivity: Design, fabrication and performance of a pig-tailed integrated optical phase-modulated mach–zehnder interferometer system," *Sens. Actuators B, Chem.*, vol. 61, no. 1, pp. 100–127, 1999.

[7] F. Prieto, A. Llobera, A. Calle, and L. M. Lechuga, "Design and analysis of silicon antiresonant reflecting optical waveguides for evanscent field sensor," *J. Lightw. Technol.*, vol. 18, no. 7, p. 966, Jul. 2000.

[8] K. Zinoviev, L. G. Carrascosa, J. S. del Río, B. Sepúlveda, C. Domínguez, and L. M. Lechuga, "Silicon photonic biosensors for lab-on-a-chip applications," *Adv. Opt. Technol.*, vol. 2008, pp. 383927-1–383927-6, Apr. 2008.

[9] D. Marcuse, "Mode conversion caused by surface imperfections of a dielectric slab waveguide," *Bell Syst. Tech. J.*, vol. 48, no. 10, pp. 3187–3215, 1969.

[10] F. P. Payne and J. P. R. Lacey, "A theoretical analysis of scattering loss from planar optical waveguides," *Opt. Quant. Electron.*, vol. 26, no. 10, pp. 977–986, 1994.

[11] T. Barwicz and H. Haus, "Three-dimensional analysis of scattering losses due to sidewall roughness in microphotonic waveguides," *J. Lightw. Technol.*, vol. 23, no. 9, pp. 2719–2732, Sep. 2005.

[12] B. S. Ahluwalia, A. Z. Subramanian, O. G. Hellso, N. M. B. Perney, N. P. Sessions, and J. S. Wilkinson, "Fabrication of submicrometer high refractive index tantalum pentoxide waveguides for optical propulsion of microparticles," *IEEE Photon. Technol. Lett.*, vol. 21, no. 19, pp. 1408–1410, Oct. 1, 2009.

[13] F. Wang, F. Liu, G.-K. Chang, and A. Adibi, "Precision measurements for propagation properties of high-definition polymer waveguides by imaging of scattered light," *Opt. Eng.*, vol. 47, no. 2, pp. 024602-1–024602-4, 2008. [Online]. Available: http://dx.doi.org/10.1117/1.2842390

[14] M. H. Jenkins, B. S. Phillips, Y. Zhao, M. R. Holmes, H. Schmidt, and A. R. Hawkins, "Optical characterization of optofluidic waveguides using scattered light imaging," *Opt. Commun.*, vol. 284, no. 16, pp. 3980–3982, 2011.